

# The effect of clay tortuosity on contaminant plume persistence

Changmin Kim<sup>1</sup>, Minjune Yang<sup>2</sup>, \*

Division of Earth Environmental System Sciences, Pukyong National University, Busan, Korea, Republic of (South)<sup>1</sup>,  
Department of Earth and Environmental Sciences, Pukyong National University, Busan, Korea, Republic of (South)<sup>2</sup>  
minjune@pknu.ac.kr

## STUDY RATIONALE

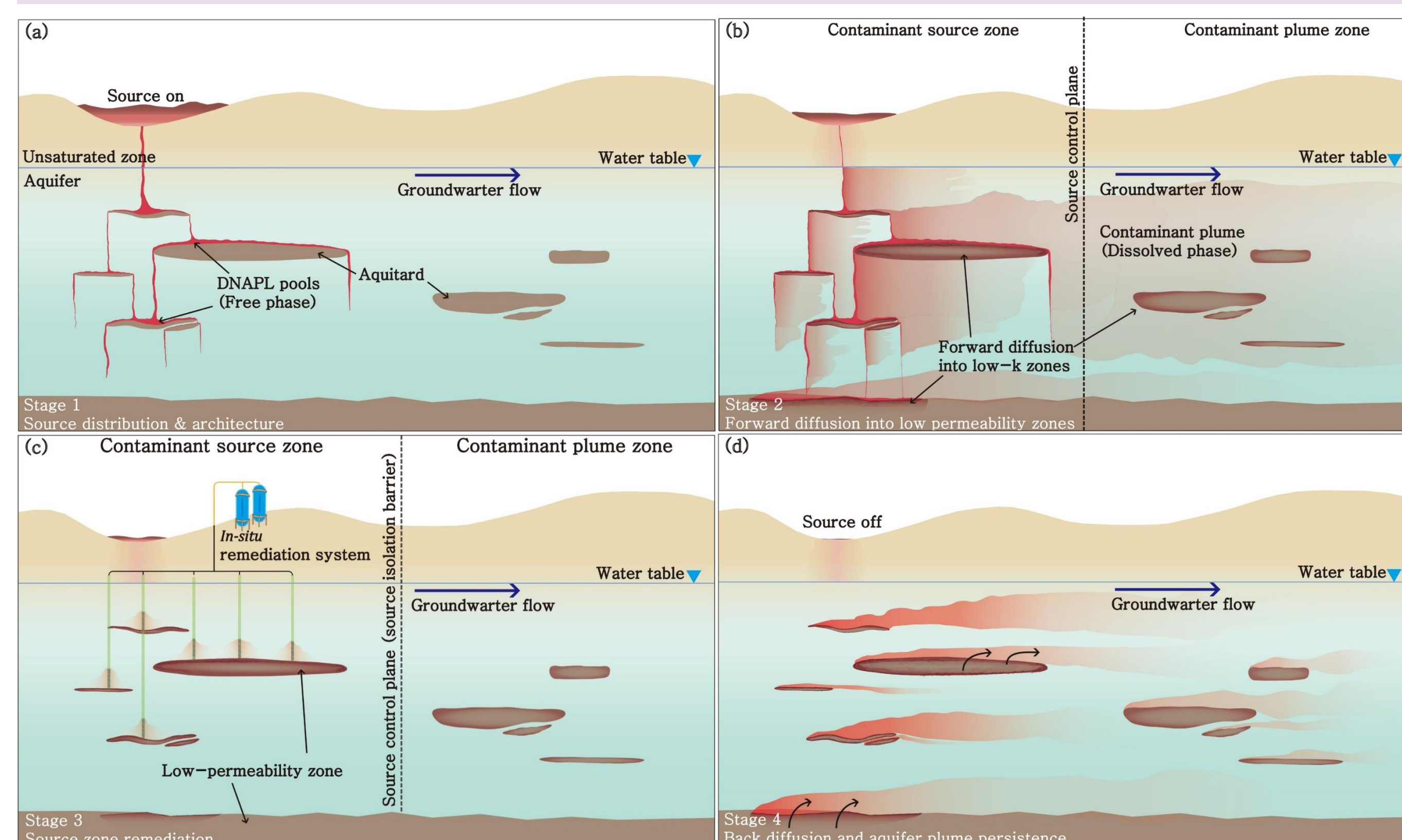


Fig. 1. Conceptual illustration of DNAPL forward and back diffusion scenario in low permeability zone. (a) Stage 1, Source distribution and architecture; (b) Stage 2, Forward diffusion into low permeability; (c) Stage 3, Source zone remediation; (d) Stage 3, Back diffusion and aquifer plume persistence.

## OBJECTIVES

**Objective 1:** to understand relative contribution of back diffusion to contaminant plume persistence depending on different clay types  
**Objective 2:** to identify the relationship between clay particle expansion and tortuosity of solute flowpath

## ANALYTICAL SOLUTIONS

The change of concentration  $C[M/L^3]$  in the aquitard with time  $t$  can be expressed by Fick's second law of diffusion.

$$\frac{\partial \eta C}{\partial t} = -\frac{\partial j}{\partial z} = \eta D^* \frac{\partial^2 C}{\partial z^2} \quad (1)$$

where  $\eta$  is the porosity of the aquitard, and  $D^*[L^2/T]$  is the effective molecular diffusion coefficient, defined as

$$D^* = \frac{D\tau}{R} = \frac{D\tau}{1 + \frac{\rho_b K_d}{\eta}} \quad (2)$$

where  $D$  is the molecular diffusion coefficient  $[L^2/T]$ ,  $R$  is the retardation factor [dimensionless],  $\rho_b$  is bulk density  $[M/L^3]$ ,  $K_d$  is the distribution coefficient  $[L^3/M]$ , and  $\tau$  is aquitard matrix tortuosity [dimensionless]. To account for a preferential solute pathway of clay matrix, tortuosity  $\tau$  is also considered.

The analytical solution for the concentration profile in a semi-infinite low-permeability zone with boundary conditions  $C(z = 0, 0 < t \leq T) = C_0$  and  $C(z = 0, t > T) = 0$ , and initial condition  $C(z > 0, t = 0) = 0$  is given by Carslaw and Jaeger (1959):

$$\frac{C(z, t)}{C_0} = f(z) - f'(z) \text{ for } t > T \quad (3)$$

$$\text{where } f(z) = \text{erfc}\left(\frac{z}{\sqrt{4D^*t}}\right), f'(z) = \text{erfc}\left(\frac{z}{\sqrt{4D^*(t-T)}}\right).$$

For the case where the diffusion front exceed over the aquitard boundary, simulation using eq (3) which assume that the aquitard depth is infinite could underestimate the solute concentration. Using the method of images, the solution for the concentration profile in a low-permeability zone of finite thickness,  $L$ , becomes

$$\frac{C(z, t)}{C_0} = [f(z) + \sum_{n=1}^{\infty} f(-z - 2nL) - f(z - 2nL)] - [f'(z) + \sum_{n=1}^{\infty} f'(-z - 2nL) - f'(z - 2nL)] \quad (4)$$

Equation (7) describes the solute concentration profile in a finite clay layer during the unloading, or back diffusion, of solutes to a high-permeability layer. Substituting eq (4) into eq (1) and differentiating results in the following expression for the back solute diffusive flux,  $j_B$ , out of a finite low-permeability zone of thickness  $L$  at the interface ( $z = 0$ ) becomes

$$j_B(z = 0, t) = C_0 \eta \sqrt{\frac{D^*}{\pi}} \left( \frac{1 + \sum_{n=1}^{\infty} (-1)^n 2 \exp g(-(2nL)^2)}{\sqrt{t}} - \frac{1 + \sum_{n=1}^{\infty} (-1)^n 2 \exp g'(-(2nL)^2)}{\sqrt{t-T}} \right) \quad (5)$$

$$\text{where } g(z) = \left(\frac{z}{4D^*t}\right), g'(z) = \left(\frac{z}{4D^*(t-T)}\right).$$

The effluent concentrations,  $C_e$ , is expressed as sum of the back diffusion flux from each of  $n$  interfaces between the aquifer and aquitard divided by the total flow through the  $m$  aquifer.

$$C_e = \frac{\sum_{i=1}^n j_{B,i} A_{i,h}}{q \sum_{j=1}^m A_{j,v}} \quad (6)$$

where  $A_{i,h}$  is the interfacial area between the aquifer and aquitard  $[L^2]$ ,  $q$  is the Darcy flux  $[L/T]$ , and  $A_{j,v}$  is the cross-sectional area of the aquifer  $[L^2]$ .

## EXPERIMENTAL METHODS

Three flow chambers with different clays (kaolinite, montmorillonite, and bentonite) were prepared respectively for 2-D diffusion experiments to verify the relative contribution of each clay type.

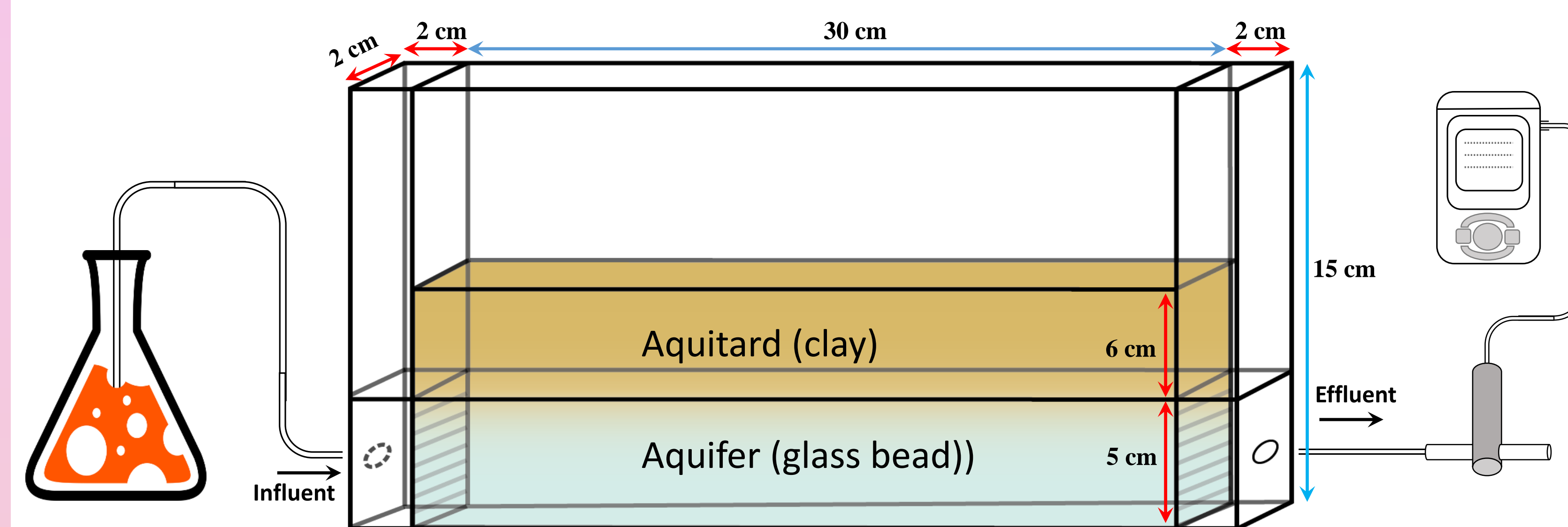


Fig. 2. Schematic of 2-D flow chamber system for forward and back diffusion experiment with bromide solution and E.C. meter.

The chambers were filled with 6 cm clay layer as an aquitard underlain by 5 cm glass bead as an aquifer. Bromide (1 g/L) as non-reactive tracer solution was injected for approximately 4 PVs. Subsequently, DI water was flushed for approximately 10 PVs to evaluate the relative contribution of back diffusion to plume persistence. The measured concentrations were compared with the 1-D analytical solution to obtain the appropriate influential parameters.

Table 3. Input parameters for analytical solutions

Parameter	Symbol	Value	Units
Diffusion coefficient	$D_0$	$4.04 \times 10^{-4}$	$m^2/d$
Retardation factor	$R$	1	-
Aquitard porosity	$\eta$	0.6	-
Aquitard depth	$z$	6	cm
Influents initial concentration	$C_0$	200	mg/L
Interfacial area	$A_{i,h}$	60	$cm^2$
Flow rate	$q$	0.17	ml/min
Cross sectional area	$A_{j,v}$	10	$cm^2$
Tortuosity of kaolinite	$\tau_k$	0.25	-
Tortuosity of montmorillonite	$\tau_m$	0.15	-
Tortuosity of bentonite	$\tau_b$	0.95	-

Molecular diffusion coefficients, porosity, and retardation factor were obtained from literature. Tortuosity values were fit to experimental results.

## RESULTS AND DISCUSSION

- The bromide effluent concentration are shown in Figure (3), illustrating the effect of general BTC plume tailing behavior after source loading was completed (11.3 PVs). The measured and simulated effluent concentrations from all three clay types were in good agreement ( $E = 0.92$  based on kaolinite, montmorillonite, and bentonite)

- Tortuosity,  $\tau$  was determined by trial and error adjustment to best fit with the experimental results. The tortuosity values were largest in bentonite ( $\tau = 0.95$ ) and smallest ( $\tau = 0.15$ ) in montmorillonite which was correspondence with the amount of mass inside the aquitard layer.

- In the diffusion experiment, the volume of all three aquitards was the same ( $V = 240 \text{ cm}^3$ ) but different mass inside. For montmorillonite, which has 150.8 g, showed the smallest tortuosity value while bentonite, which has only 15.93 g of clay, showed the largest tortuosity value.

- The bentonite tortuosity value of 0.95 which close to 1 was similar to that of solute diffused in the water. It was considered that bentonite particle expanded and space between interlayers are almost saturated, forming colloid matrix, resulting water-like solute pathway.
- The amount of kaolinite inside the chamber was smaller than that of montmorillonite as 135.39 g which is correspondence with the larger tortuosity value of kaolinite. The larger density of aquitard, the more complicate of solute flow path, resulting smaller tortuosity value.

- Tortuosity was generally defined as the ratio of straight-line distance and tortuous flowpath length. However, tortuous solute pathway was strongly affected by the mass inside the aquitard and its expansion characteristics which should be used as key factor of tortuosity

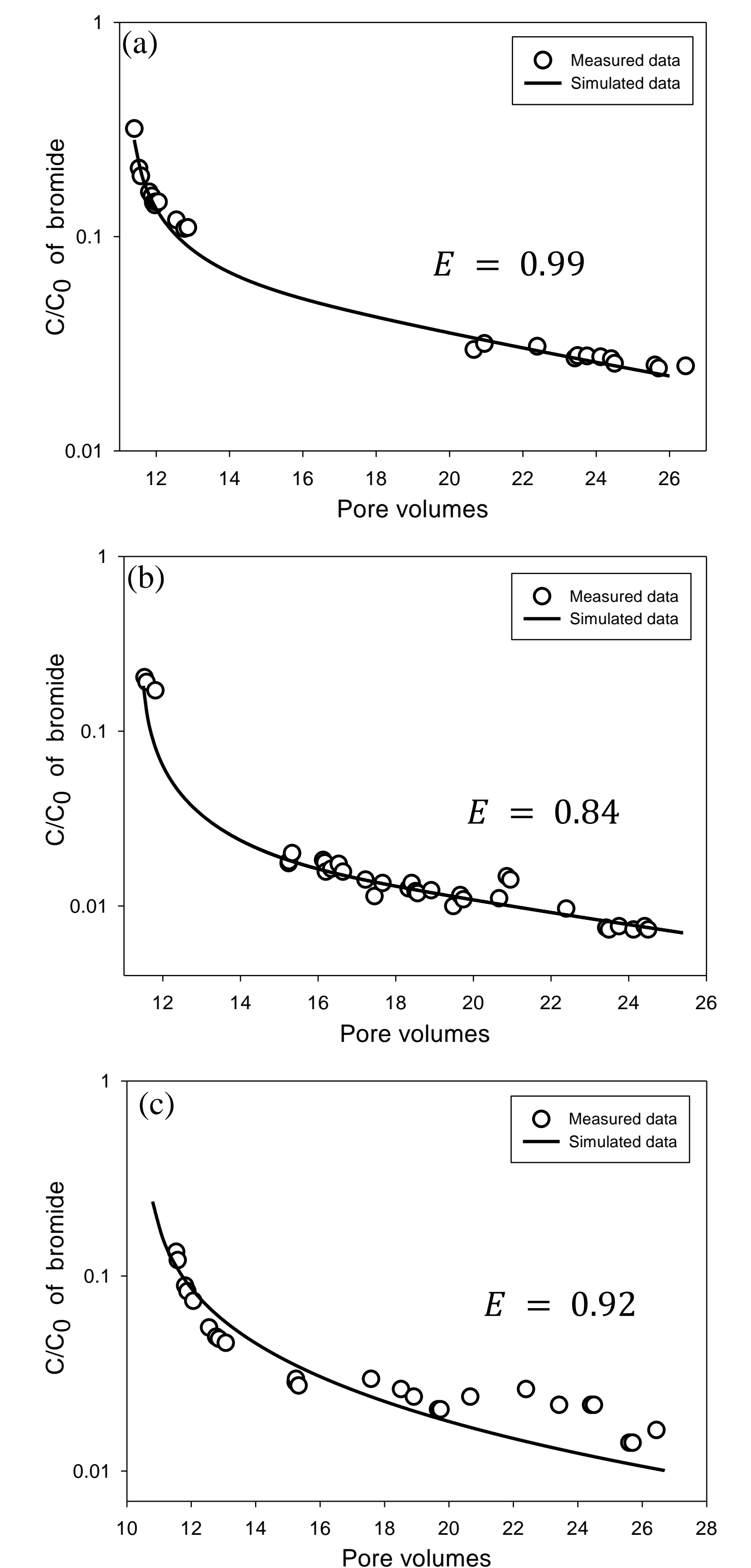


Fig. 3. Measured (circle) breakthrough curves and simulated (line) tailings for bromide in (a) kaolinite, (b) montmorillonite, and (c) bentonite.